Available online at www.sciencedirect.com
ScienceDirect
Journal of Sound and Vibration 325 (2009) 34–48
JOURNAL OF SOUND AND VIBRATION
www.elsevier.com/locate/jsvi

Horizontal shaking table tests on structures using innovative earthquake mitigation devices

Zhao-Dong Xu[a,b,*]

[a]*Civil Engineering College, Southeast University, Si-Pai Lou 2#, Nanjing 210096, China*
[b]*RC&PC Key Laboratory of Education Ministry, Nanjing, China*

Received 10 November 2008; received in revised form 18 February 2009; accepted 14 March 2009
Handling Editor: L.G. Tham
Available online 18 April 2009

Abstract

Viscoelastic (VE) devices have been widely used to mitigate the dynamic responses of the structures resulting from the earthquake or the strong wind for more than 20 years. These devices are usually installed in the upper portion of the structures to reduce the vibration responses. Few devices, however, are attempted to mitigate and isolate multidimensional vibration energy at the same time. In this paper, an innovative device, multidimensional earthquake isolation and mitigation device (MEIMD), is proposed, which can perform its ''name-giving'' task of earthquake isolation and earthquake mitigation simultaneously. In order to fully quantify the earthquake isolation and mitigation effects on structures equipped with the MEIMD, the following tasks are performed. Firstly, shaking table tests on steel frame structures with and without the devices are carried out. Secondly, based on the recorded data of the acceleration and displacement responses of the tested structures, the analysis of dynamic characteristics is performed. Finally, a comparison between the finite element analytical and experimental results for the test structure is presented. All of results, on the one hand, illustrate that the finite element numerical results are accordant with the experimental results; on the other hand, they demonstrate that the devices not only have remarkable earthquake isolation action but also have fine mitigation effect in horizontal direction.

1. Introduction

Protection of civil engineering structures from damages induced by seismic activity or strong winds has become an increasingly critical issue. Various structural control means have been developed and implemented over the years to mitigate the dynamic responses of structures. Such devices include viscoelastic (VE) dampers, viscous dampers, metallic yield dampers, tuned mass dampers, earthquake isolation devices, and kinds of active control devices [1–3]. Earthquake isolation devices and shock absorption devices are commonly employed in real applications presently. Examples of these earthquake isolation devices include rubber bearing, the slip friction bearing, the roll bearing, and the swing bearing [4]. However, these earthquake isolation devices can only isolate transmission of vibration energy, and cannot dissipate vibration energy.

*Corresponding author at: Civil Engineering College, Southeast University, Si-Pai Lou 2#, Nanjing 210096, China.
E-mail address: xuzhdgyq@seu.edu.cn

0022-460X/$ - see front matter © 2009 Elsevier Ltd. All rights reserved.
doi:10.1016/j.jsv.2009.03.019

Few researches have been done involving devices having both earthquake isolation ability and earthquake mitigation ability [5].

VE material is a high molecule polymer possessing incredible ability of energy dissipation and energy storage, in other words VE material contains characteristics of both spring and fluid. VE dampers are the ordinary devices for mitigating dynamic responses. This is accomplished by making full use of energy dissipation ability of VE material. Most of research was primarily focused on properties of VE dampers and dynamic responses analysis for the structures with VE dampers. A few dynamic tests on the structures with VE dampers were carried out to verify the effectiveness of this kind of device. Dynamic behavior of a prototype and a 2/5 scaled five-floor steel frame structures with VE dampers was experimented [6]. Experimental study on seismic behavior of 1/4 scaled three-floor viscoelastically damped steel frame structure was performed [7]. Shaking table tests on 1/3 scaled three-floor reinforced concrete structure with VE dampers were carried out [8]. Seismic behavior of a 2/5 scaled five-floor steel frame structure with VE dampers was experimented [9]. Seismic behavior of a 2/5 scaled three-floor steel frame structure with VE dampers was tested [10]. Dynamic behavior of a 1/8 scaled 16-floor steel frame structure with VE dampers was tested [11]. Dynamic tests on seismic behavior and structural integrity characteristic on 1/3 scaled three-floor reinforced concrete structure with VE dampers were carried out [12]. The earthquake mitigation effectiveness of VE dampers for structures has been verified through the vibration test on a five-storey steel frame [13]. Seismic responses of full-scale structure with VE dampers were experimentally verified to be reduced effectively [14]. Several VE dampers were installed in weak-layer floors of five-floor steel frame structures to reinforce the anti-earthquake ability of structures by shaking table tests [15].

In this paper, the multidimensional earthquake isolation and mitigation device (MEIMD), which consists of VE bearing, VE dampers, springs, and connection devices, was proposed based on fine energy dissipation ability of VE material. Furthermore, the MEIMD can perform the tasks of earthquake isolation and earthquake mitigation simultaneously. In order to verify earthquake isolation and mitigation effect of the devices on structures, the following tasks are performed. Firstly, shaking table tests on 1/3 scaled three-floor steel frame structures with and without the devices are carried out. Secondly, based on the recorded data of the acceleration and displacement responses of the tested structures, the analysis of dynamic characteristics is performed. Finally, a comparison between the finite element analytical and experimental results for the test structure is presented. All of results, on the one hand, illustrate that the finite element numerical results fit well with the experimental results; on the other hand, they demonstrate that the devices not only have remarkable effects on the earthquake isolation action but also have obvious mitigation effects.

2. Test set-up

2.1. Property for MEIMD

The proposed MEIMD (with patent granted number ZL 03 113392.4) is made up of one core VE bearing and several VE dampers, as shown in Fig. 1. One innovative idea for this device is adopting VE energy dissipation material to substitute traditional rubber in the core bearing. Obviously VE bearings are superior to the ordinary rubber bearing in earthquake mitigation aspect due to the excellent energy dissipation ability of VE material. Another innovative idea for this device is the vertical earthquake isolation and mitigation system which consists of dampers, bearing, and springs, and the mechanism for earthquake isolation and mitigation of the device in vertical direction. The relative shaking table tests will be introduced in other paper due to the length limit of the paper. The emphasis of this paper will be on the horizontal earthquake isolation and mitigation research. Under the horizontal earthquake excitation, the device can isolate earthquake energy and prevent vibration energy from transferring to the upper structure like a rubber bearing. At the same time, the VE dampers and the core VE bearing can dissipate the input earthquake energy due to their horizontal relative deformations of VE layers.

The properties tests including energy dissipation curves and fatigue characteristics changing with excitation frequency, temperature, excitation amplitudes were carried out before the shaking table tests in the RC and PC State Education Ministry Key Laboratory in Southeast University, China. Experimental and numerical study on the devices will be introduced in other paper in detail. Here tests description, working principle and

Fig. 1. Multidimensional earthquake isolation and mitigation device.

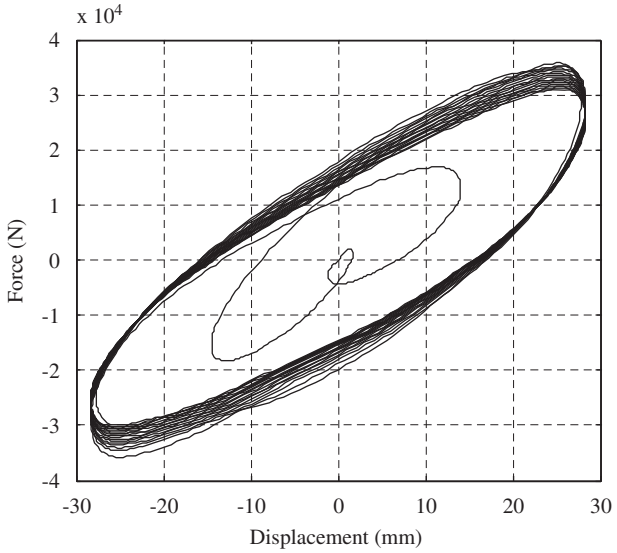

Fig. 2. The hysteresis curves of the device.

energy dissipation curves are only introduced briefly. Horizontal and vertical property tests were carried out for the device. The core bearing consists of 35 viscoelastic layers with the thickness of 3 mm for each layer vulcanized intervally with 34 layers of 2 mm steel plates. The diameter and the height of the core bearing are 70 and 173 mm, respectively. Take horizontal tests for an example, four excitation frequencies (0.1, 0.2, 0.5, 1 Hz) and two excitation amplitudes (10 and 20 mm) are considered in this tests. Each test consists of 20 cycles of sinusoidal excitation with a fixed displacement amplitude and excitation frequency. Test duration of 20 cycles is chosen as representative of the duration of building response up to a severe level earthquake. Outputs from the actuator load cell and displacement transducer are recorded by a high speed digital data acquisition system. As shown in Fig. 2, the force–displacement hysteresis curves of the device are saturated ellipses under the horizontal sinusoid excitations, which shows the device has excellent horizontal energy dissipation capabilities. The mathematical model can be simulated by Kelvin model.

2.2. *The model structure design and loading program*

In order to verify the effectiveness of the MEIMD, shaking table tests on the model frame structures with and without the devices are carried out. The test frame models are two identical 1/5-scale three-storey plain

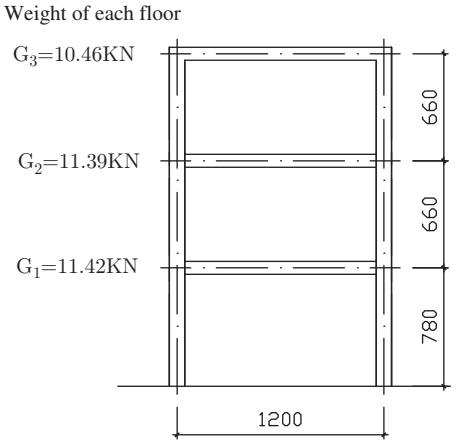

Fig. 3. Schematic of the model frame.

Fig. 4. Shaking table tests on the structure.

steel frames, i.e. the model scale factor $S_l = 0.2$. In order to strengthen the stability of the frame and to facilitate adding weights, two identical frames are adopted. As shown in Fig. 3, a lumped mass system with weights of 11.42 KN for the first floor, 11.39 KN for the second floor, and 10.46 KN for the top floor is used to simulate the prototype structure. The overall dimensions of each test frame are 1.2 m in span with storey heights of 780 mm for the first storey and 660 mm for the other two, as also shown in Fig. 3. The beams and columns adopt I 10 steel. The bottom of each column is welded on the upper steel plate of the MEIMD, and the bottom steel plate of the device are connected to the table-board by bolts. Fig. 4 shows the test structures installed on the shaking table. The upper steel plate and the bottom steel plate of each MEIMD can be fixed by the six bolts. When bolts are removed, the devices will work, and the controlled structure with devices will be experimented on. However, when the bolts are put into their places, the devices will be fixed and not work. This allows for experiments for the uncontrolled structure without the use of the devices. Four accelerators are adopted, which are fixed on the each floor of the frame structure and the table-board. To measure displacement responses one displacement sensor is installed in each floor.

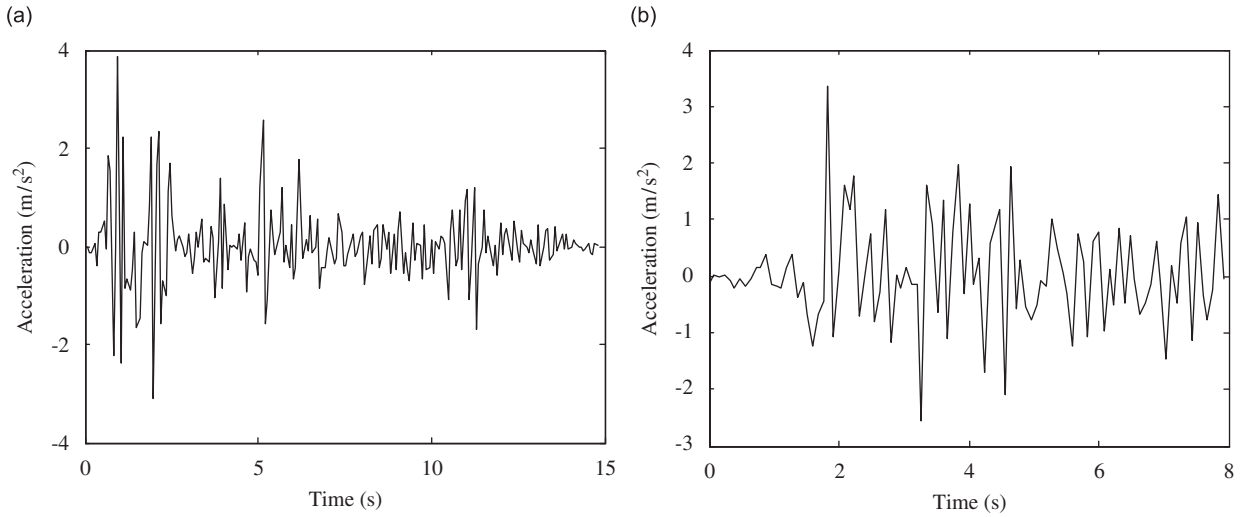

Fig. 5. Earthquake excitation waves: (a) El Centro wave and (b) Taft wave.

Table 1
The loading program of the shaking table tests.

No.	Name	Waves	Magnitude (gal)	Condition
1	R1	White noise	200	Uncontrolled
2	LT1	Taft	120	Uncontrolled
3	LE1	El Centro	120	Uncontrolled
4	E1	El Centro	120	Controlled
5	T1	Taft	120	Controlled
6	LT2	Taft	240	Uncontrolled
7	LE2	El Centro	240	Uncontrolled
8	E2	El Centro	240	Controlled
9	T2	Taft	240	Controlled
10	LE5	El Centro	400	Uncontrolled
11	R2	White noise	200	Uncontrolled
12	R3	White noise	200	Controlled
13	E5	El Centro	400	Controlled
14	E7	El Centro	600	Controlled
15	E8	El Centro	800	Controlled
16	R4	White noise	200	Controlled

The tests were carried out in Dynamic Laboratory of Hohai University, China. Firstly white noise excitation tests were adopted to measure the natural frequencies, mode shapes and damping ratios before earthquake excitations. El Centro and Taft earthquake waves as shown in Fig. 5 with peak values of 120, 240, 400, 600, and 800 gal were adopted as excitations for shaking table test, then white noise excitation tests were carried out to determine changes of dynamic characteristics of the model structure, and the loading program can be seen in Table 1 in detail. It must be noted that "uncontrolled" in Table 1 means the structure does not adopt the MEIMD and "controlled" means the structure adopts the devices.

3. Test results and analysis

3.1. Dynamic characteristics

In order to get the dynamic characteristics including natural frequencies, damping ratios and mode shapes of the model structures with or without MEIMD, four white noise excitation tests are carried out. As shown in

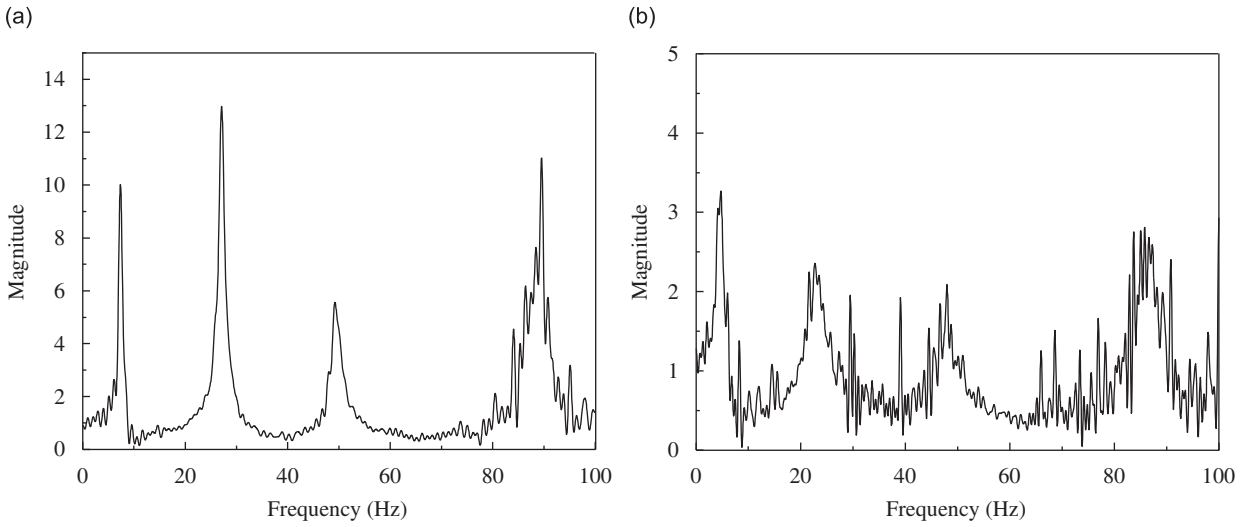

Fig. 6. Frequency-spectra analysis for the acceleration responses: (a) frequency-spectra of the R1 test and (b) frequency-spectra of the R3 test.

Table 1, R1 is the test of dynamic characteristics of the structure without MEIMD before all tests, R2 is the test of dynamic characteristics of the structure without MEIMD after some minor excitation tests, R3 is the test of dynamic characteristics of the structure with MEIMD before strong excitation tests, and R4 is the test of dynamic characteristics of the structure with MEIMD after strong excitation tests. Frequency-spectra analysis is carried out for acceleration responses of each floor, and magnitude-frequency and phase-frequency relationships of acceleration responses are obtained by using transformation function and fast Fourier transformation technique [12,16]. Fig. 6(a) and (b) show the results of frequency-spectra analysis for the acceleration responses of the top floor of the structures with and without devices, respectively. The frequency corresponding to the peak value in magnitude-frequency figure is the natural frequency, and the damping ratio can be determined by half-brand method [12,16]. The tested natural frequencies and damping ratios are listed in Table 2. It can be seen from Table 2 that the first natural frequency of the model structure decreases clearly when the MEIMD are installed. The first natural frequency of the structure with devices is 4.728 Hz, i.e. the result of the third white noise excitation test. Comparing with the first frequency of the structure without devices (7.381 Hz, i.e. the result of the first white noise excitation test) to the first natural frequency of the structure with devices, resulting in frequency of 2.653 Hz; this is a decrease by 35.94%. This shows that the natural period of the structure is extended when the MEIMD are adopted. In fact, this is induced by the earthquake isolation effect of the devices. At the same time, it can be also shown from Table 2 that the damping ratios of the structure increase obviously when the MEIMD are adopted. For example, the first damping ratio of the structure without devices is 4.69%, and that of the structure with devices is 14.80%; therefore, there was an increase by 215.56%. The increase of the damping ratio shows that the devices have significant earthquake mitigation ability under the horizontal earthquake excitation. The above analysis is based on the idea that the stiffness of the structure, the natural frequency and the damping ratio are usually increased when the earthquake mitigation devices are working. Additionally, the natural period is usually increased and the damping ratio changes slightly when the MEIMD are installed in structures. Some sub-peaks are found near the second and the third frequencies in frequency-spectra figures, as shown in Fig. 6. Thus it is difficult to obtain the damping ratios under the second and third modes. But it can be seen from Fig. 6 that breadth of the peaks becomes broad at the first, second, and third frequencies when the devices are installed in the structure. This shows the damping ratios of all modes are increased. At the same time, the peak values at all frequencies reduced clearly, which shows the dynamic responses are reduced when the devices are installed in the structure.

Table 2
The tested dynamic characteristics.

Name	Dynamic characteristics	The first mode	The second mode	The third mode
R1	Frequency	7.381	27.13	49.16
	Damping ratio	4.69%	–	–
R2	Frequency	7.194	26.6	48.84
	Damping ratio	4.19%	–	–
R3	Frequency	4.728	22.34	48.67
	Damping ratio	14.80%	–	–
R4	Frequency	4.289	22.05	45.91
	Damping ratio	13.86%	–	–

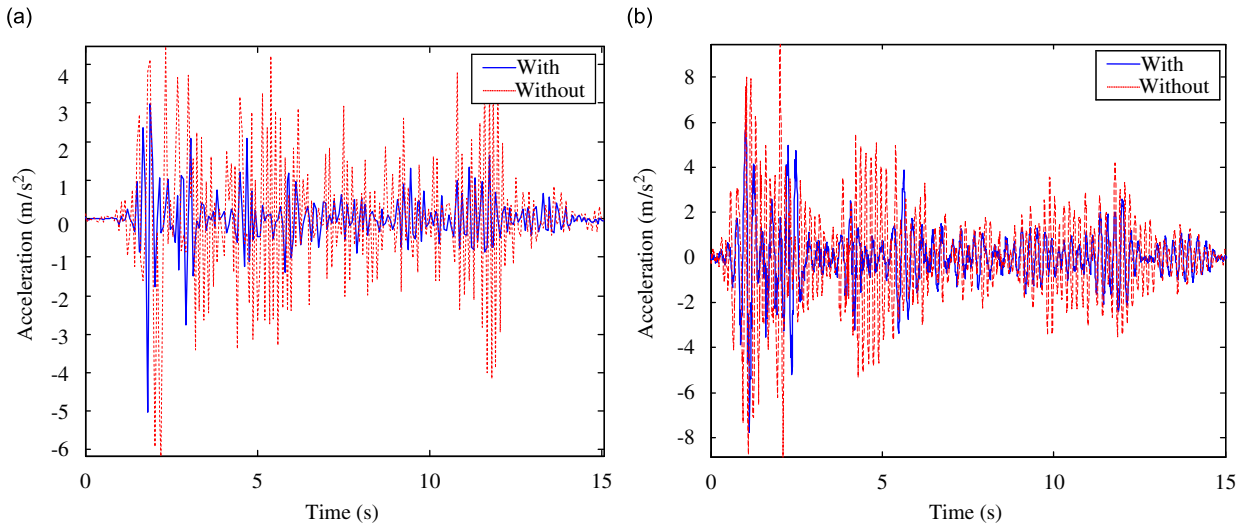

Fig. 7. Comparison of acceleration responses between the structures with and without devices: (a) the first floor and (b) the top floor.

3.2. Acceleration responses

To better visualize the earthquake isolation and mitigation effect of the devices, the acceleration responses of the structures with and without devices are compared. Fig. 7 shows the acceleration responses comparison of the first floor and the top floor relative to that of the table-board under 400 gal El Centro earthquake excitation. It can be seen from Fig. 7 that the acceleration responses of the structure with devices are clearly smaller than those of the structure without devices. The maximum acceleration response of the top floor of the structure without devices is 8.877 m/s^2, while that of the structure with devices is 7.084 m/s^2, which is a decrease by 20.20%. The maximum acceleration response of the first floor of the structure without devices is 6.156 m/s^2, while that of the structure with devices is 5.036 m/s^2, which is a decrease by 18.19%. Table 3 lists the maximum acceleration response of each floor relative to table-board for structures with and without devices under different loading conditions. The numerical data in Table 3 are obtained by the finite element method described in the following section. It can be seen that the acceleration responses are reduced significantly in other earthquake excitations when the MEIMD are installed in the structure. For example, under the 240 gal Taft earthquake excitation, the maximum acceleration responses of the first, second, and top floors of the structure without devices are 2.280, 5.044, and 5.665 m/s^2, respectively. While those for the structure with devices are 2.045, 2.990, and 3.335 m/s^2, which is decreased by 10.31%, 40.72%, and 41.13%,

Table 3
Comparison of acceleration of each floor relative to table-board.

Excitation		Without devices (m/s^2)			With devices (m/s^2)		
		Num.	Exp.	Error (%)	Num.	Exp.	Error (%)
El Centro							
120 gal	Top	2.968	3.109	4.54	2.279	1.892	16.98
	Second	2.872	2.392	16.71	2.065	1.577	23.63
	First	1.748	2.004	12.77	1.754	1.453	17.16
240 gal	Top	5.894	6.135	3.93	4.215	4.079	3.22
	Second	5.341	4.654	12.86	3.870	3.580	7.49
	First	2.938	3.272	10.21	3.141	3.163	0.70
400 gal	Top	8.993	8.877	1.29	6.934	7.084	2.12
	Second	8.074	8.185	1.36	6.017	6.203	3.00
	First	5.678	6.156	7.76	4.941	5.036	1.89
800 gal	Top	–	–	–	11.443	13.438	14.85
	Second	–	–	–	9.814	11.572	15.19
	First	–	–	–	8.727	10.206	14.49
Taft							
120 gal	Top	2.358	2.977	20.79	1.306	1.782	26.71
	Second	1.761	2.319	24.06	1.226	1.533	20.02
	First	1.368	1.801	24.04	1.061	1.278	16.98
240 gal	Top	5.204	5.665	8.14	2.887	3.335	13.43
	Second	4.640	5.044	8.01	2.500	2.990	16.39
	First	2.080	2.280	8.77	2.027	2.045	0.88

respectively. The average value of all decreasing percentages under all earthquake excitations for the maximum acceleration responses of the first, the second and the top floors listed in Table 3 is 27.90%. All these indicate that the VE devices have good earthquake isolation and mitigation effects on the structure. It can be also seen from the experimental results under all loading conditions that the dynamic responses are reduced more clearly under Taft earthquake excitation than under El Centro earthquake excitation.

3.3. Displacement responses

Displacement data of all floors of the structure with devices are compared with those of the structure without devices under different loading conditions. Fig. 8 shows comparison of the displacement responses of the first floor and the top floor relative to that of the table-board under 400 gal El Centro earthquake excitation. It can be shown from Fig. 8 that the displacement responses are reduced obviously and the time history curves become mild when the MEIMD are installed in the structure. The maximum displacement response of the top floor of the structure without devices is 3.20 mm, while that of the structure with devices is 2.20 mm, which is decreased by 31.25%. The maximum displacement response of the first floor of the structure without devices is 1.31 mm, while that of the structure with devices is 1.08 mm. This is a decrease by 17.56%. The maximum displacement responses of all floors, as seen in Table 4, relative to that of the top plates of MEIMD under different earthquake excitations. It must be noted that the displacement responses under 600 and 800 gal El Centro earthquake excitations do not appear in Table 4 because the displacement sensors become flexible. In the same manner, the numerical data in the table are obtained by the finite element method described in the following section. It can be seen from Table 4 that the displacement responses of all floors are reduced obviously for the structures with MEIMD under different loading conditions. For instance, under the 240 gal El Centro earthquake excitation, the maximum relative displacement responses of the first floor, the second floor, and the top floor for the structure without devices are 1.11, 1.78, and 2.21 mm, while those for the structure with devices are 0.68, 1.20, and 1.43 mm. This results in reductions by 38.74%, 32.58%,

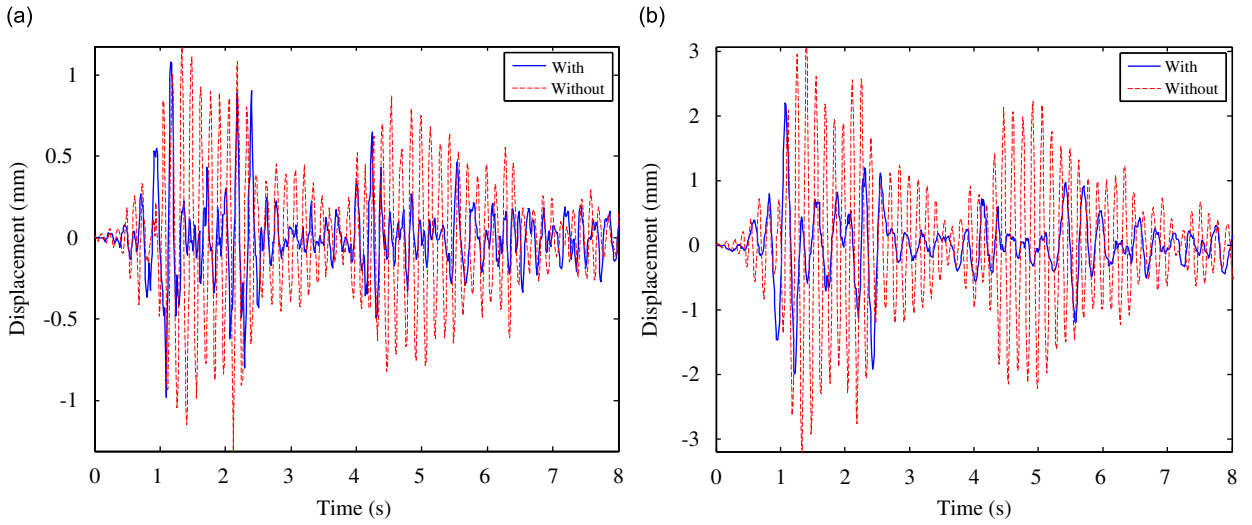

Fig. 8. Comparison for displacement responses under 400 gal El Centro earthquake excitation: (a) the first floor and (b) the top floor.

Table 4
Comparison of displacement of each floor relative to top of the devices.

Excitation	Without devices (mm)			With devices (mm)		
	Num.	Exp.	Error (%)	Num.	Exp.	Error (%)
El Centro						
120 gal						
Top	1.05	1.39	24.46	0.70	0.80	12.50
Second	0.82	1.01	18.81	0.56	0.71	21.26
First	0.49	0.47	4.08	0.33	0.34	2.94
240 gal						
Top	1.96	2.21	11.31	1.39	1.43	2.80
Second	1.56	1.78	12.35	1.11	1.20	7.50
First	0.94	1.11	15.31	0.65	0.68	4.41
400 gal						
Top	3.01	3.20	5.94	2.33	2.20	5.58
Second	2.43	2.48	2.01	1.87	1.85	1.07
First	1.47	1.31	10.88	1.10	1.08	1.82
Taft						
120 gal						
Top	0.97	0.96	1.03	0.62	0.67	7.46
Second	0.77	0.81	4.93	0.49	0.59	16.95
First	0.46	0.46	0	0.29	0.21	27.58
240 gal						
Top	2.19	2.54	13.78	1.21	1.21	0
Second	1.74	2.06	15.53	0.97	1.09	7.34
First	1.04	1.16	10.34	0.57	0.55	3.51

and 35.29%, respectively. Through statistical analysis, comparison of the displacement responses of the first, second and top floors for the structure without devices, compared with those with devices are reduced by 52.59%, 47.09%, and 50.68%, respectively, under 240 gal Taft earthquake excitation. The average value of all

decreasing percentages under all earthquake excitations for the maximum displacement responses of the first, the second, and the top floors listed in Table 4 is 36.29%. It can be further concluded that the VE devices have better horizontal earthquake isolation and mitigation effects under Taft earthquake excitation than El Centro earthquake excitation.

4. Comparison between experimental and numerical results

4.1. Numerical model

The model of the structure in shaking table tests includes two parts: one is the upper structure, three-storey plane steel frame with total height of 2100 mm and bay of 1200 mm, and the other is the MEIMD. Material of the model is steel except for the VE devices. The finite element models are established for the structure with and without isolation and mitigation devices, respectively. In the process of modeling, Kelvin model is used to simulate the damping element, i.e. the dashpot element is paralleled with the spring element, the parameters of the dashpot and the spring elements can then be determined by the performance tests [17].

4.2. Dynamic characteristics comparison

As described before, the frequency-spectra curves of acceleration responses of all floors can be plotted in accordance with experimental data. By doing this, the relationship of phase angle differences between the input and output values changing with frequency can be obtained from phase frequency characteristic diagram of the frequency-spectra curves [16]. Considering the peak values of acceleration responses of all floors under the same natural frequency and the corresponding phase relationship, mode shapes of the model structures

Table 5
Comparison of natural frequencies between experimental and numerical results.

The structure without devices				The structure with devices			
Mode	1 (Hz)	2 (Hz)	3 (Hz)	Mode	1 (Hz)	2 (Hz)	3 (Hz)
Numerical	7.807	26.39	46.62	Numerical	4.421	29.92	54.88
Experimental	7.288	26.86	49.00	Experimental	4.508	22.2	47.29

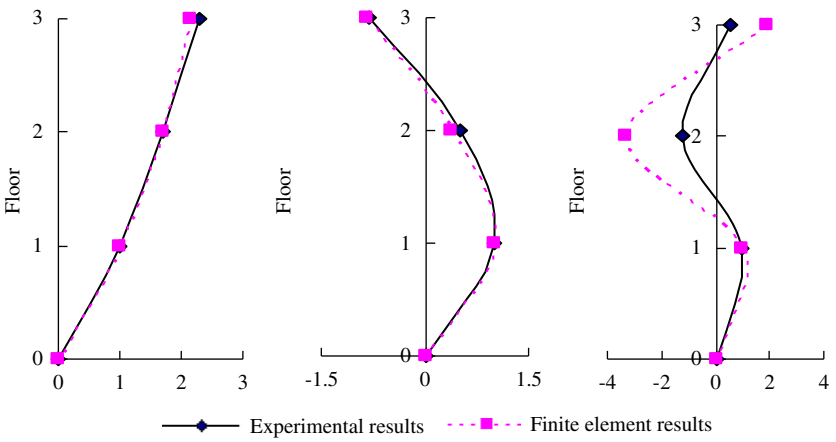

Fig. 9. Comparison of mode shapes for the structure without devices.

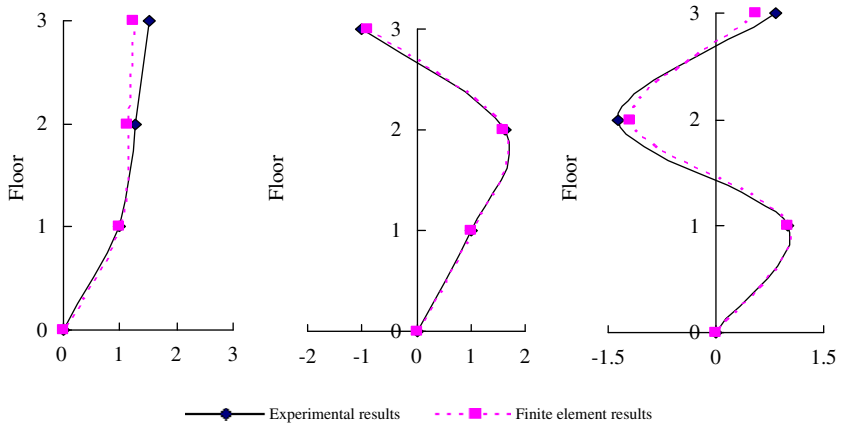

Fig. 10. Comparison of mode shapes for the structure with devices.

with and without VE devices can be obtained. At the same time, mode shapes and natural frequencies of the model structures with and without devices can be calculated by the finite element analysis. Table 5 presents the comparison of natural frequencies between the numerical and experimental results. Fig. 9 shows comparison of mode shapes between the numerical and experimental results for the model structure without devices. A comparison of mode shapes between the numerical and experimental results, shown in Fig. 10, for the model structure with devices.

It can be seen from the finite element numerical and experimental results that the difference of the first natural frequency between numerical and experimental results is minor. The differences of the second and third frequencies, however, are greater than that of the first mode. For instance, the experimental and numerical first frequencies for the structure without devices are 7.288 and 7.807 Hz. The experimental and numerical first frequencies for the structure with devices are 4.508 and 4.421 Hz. Usually, the order of the mode is higher, the natural frequency of this order is more difficult to be obtained by tests, and the error between experimental and numerical results is more obvious [18]. It is also can be seen that the numerical mode shapes fit well with the experimental results except for the third mode of the structure without devices. Comparisons of dynamic characteristics show the finite element model can describe the tested model structures, choice of parameters and simulation of the devices are demonstrated to be sound.

4.3. Acceleration responses comparison

In order to check the accuracy of numerical results, numerical acceleration responses of all floors for structures with and without devices are compared with experimental results. Fig. 11(a) and (b) show the comparison of acceleration responses of the first floor and the top floor for the structure without devices under 400 gal El Centro excitation. Fig. 11(c) and (d) show the comparison of acceleration responses of the first floor and the top floor for the structure with devices under 400 gal El Centro excitation. The maximum numerical and experimental acceleration responses and the error percentages of each floor under different excitations are listed in Table 3.

It can be found from Fig. 11 and Table 3 that the acceleration responses obtained by finite element program simulation are in good agreement with the experimental results. As shown in Fig. 11, for the structure without devices under 400 gal El Centro earthquake excitation, the numerical and experimental results of the top floor are 8.993 and 8.877 m/s^2. This leaves an error percentages is 1.29%. For the structure with devices under 400 gal El Centro earthquake excitation, the numerical and experimental results of the top floor are 6.934 and 7.084 m/s^2, the error percentages is 2.12%. As seen, the errors under the minor or major earthquakes are usually more than the errors under the moderate earthquakes. The main causes is measuring data are not precise under the minor earthquakes and the potential damages may be occurred in the structure in the major

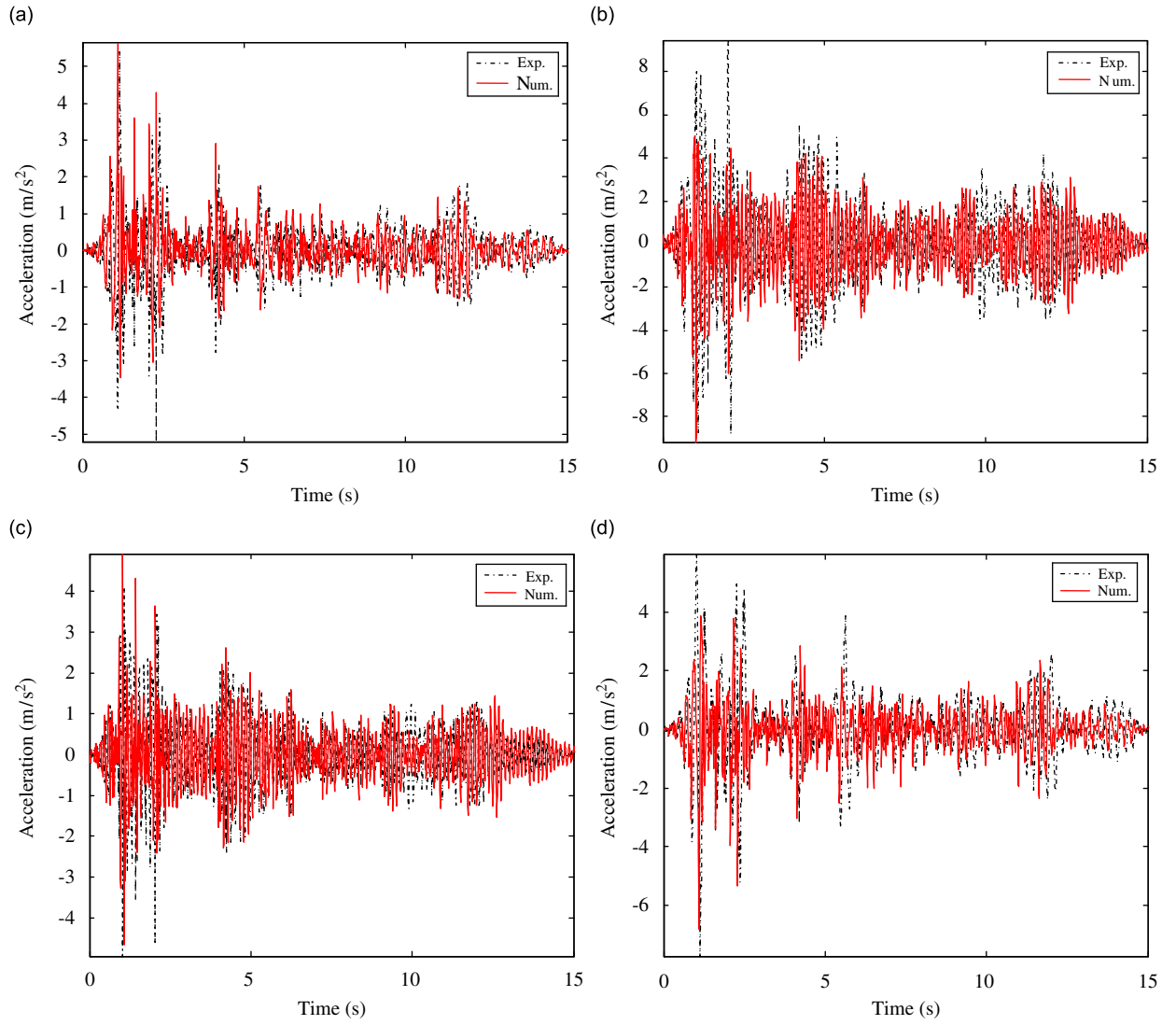

Fig. 11. Comparison of acceleration responses under 400 gal El Centro earthquake: (a) the first floor of the structure without devices, (b) the top floor of the structure without devices, (c) the first floor of the structure with devices, and (d) the top floor of the structure with devices.

earthquakes, while these damages can not be reflected in the numerical modeling. At the same time, it can be seen from Fig. 11 and Table 3 that the numerical and experimental acceleration responses are reduced obviously when the MEIMD are installed in the structure.

4.4. Displacement responses comparison

Similarly, the numerical displacement responses are compared with the experimental results. In Fig. 12(a) and (b), there are comparisons of displacement responses of the first floor and the top floor for the structure without devices under 400 gal El Centro excitation. As demonstrated by Fig. 12(c) and (d), the comparison of displacement responses of the first floor and the top floor for the structure with devices under 400 gal El Centro excitation. In Table 4, the maximum numerical and experimental displacement responses and the error percentages are listed for each floor under different excitations.

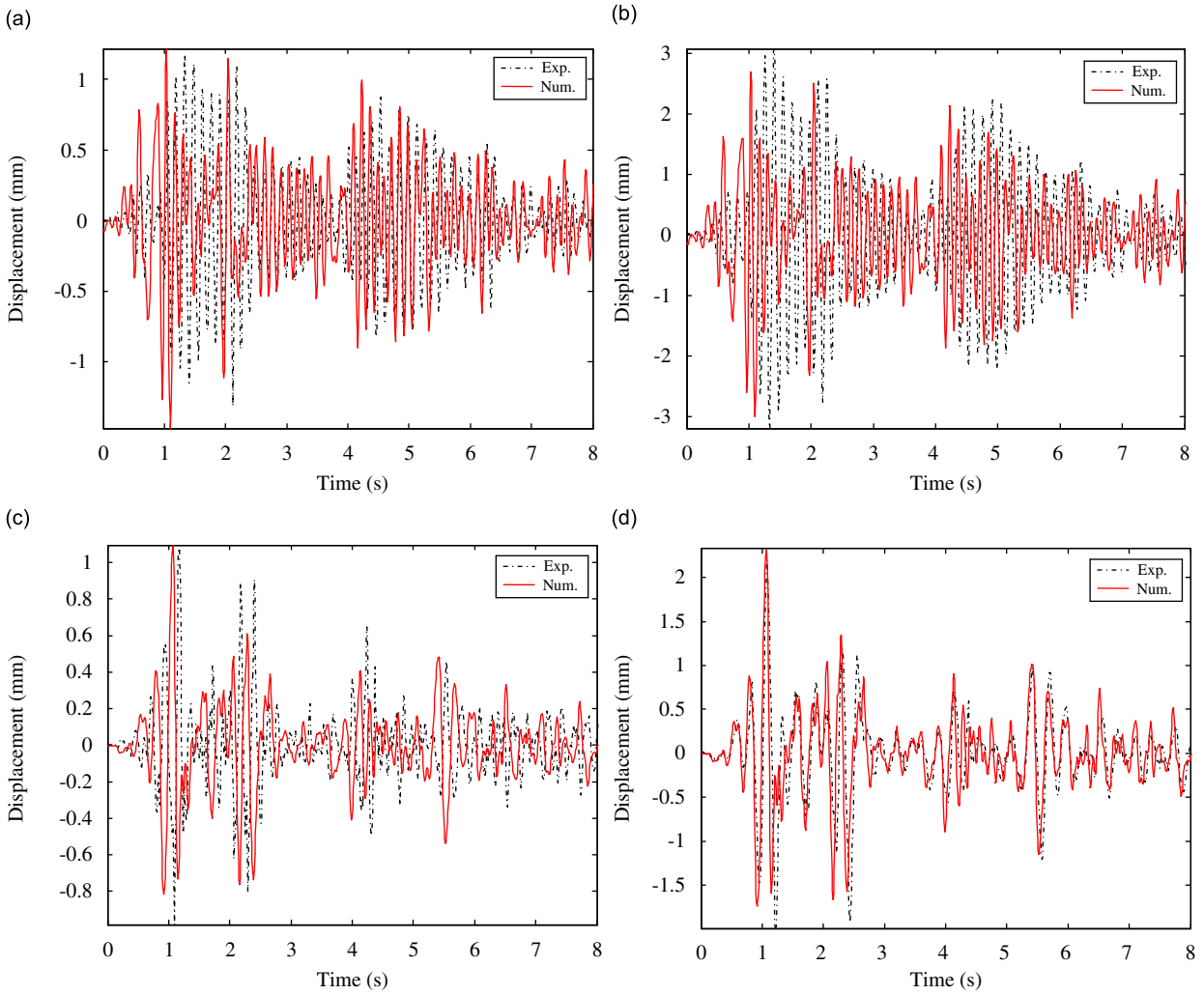

Fig. 12. Comparison of displacement responses under 400 gal El Centro earthquake: (a) the first floor of the structure without devices, (b) the top floor of the structure without devices, (c) the first floor of the structure with devices, and (d) the top floor of the structure with devices.

It can be also found from Fig. 12 that the numerical displacement time history curves fit well with the experimental results for the structures with and without devices. Under 400 gal El Centro earthquake excitation, the numerical maximum displacement responses of the first floor and the top floor for the structure without devices are 1.47 and 3.01 mm. The experimental maximum displacement responses of the first floor and the top floor are 1.31 and 3.20 mm, while the error percentages are 10.88% and 5.94%, respectively. For the structure with devices, the numerical maximum displacement responses of the first floor and the top floor are 1.10 and 2.33 mm. The experimental maximum displacement responses of the first floor and the top floor are 1.08 and 2.20 mm, while the error percentages are 1.82% and 5.58%, respectively.

The maximum displacement responses and error results listed in Table 4 verify effectiveness of the devices and exactness of the numerical modeling further. As discussed in Section 3, the numerical results show further that whatever for El Centro earthquake excitations or for Taft earthquake excitations, the maximum displacement responses are clearly reduced when the MEIMD are installed in the structure. It can be seen further from Table 4 that the calculated results of the finite element analysis fit well with experimental results.

5. Conclusions

In this paper, an innovative MEIMD is proposed. Shaking table tests and numerical analysis on the structures with and without the MEIMD are carried out. The following conclusions can be obtained from the tests and analysis:

(1) When the MEIMD are installed in the structure, the natural frequencies decrease, the damping ratios increase. Additionally, the acceleration responses will be reduced by 27.90% averagely, and the displacement responses will be reduced by 36.29% averagely. It can be concluded from the experimental results that the proposed devices are effective earthquake isolation and mitigation devices, which have fine earthquake isolation and earthquake mitigation ability in horizontal direction.
(2) The numerical dynamic characteristics, acceleration responses and displacement responses calculated by the finite element analysis fit well with the experimental results, which shows that parameters choice and model simulation are rational when erecting the finite element model. The numerical results also verify the effectiveness of the earthquake isolation and mitigation ability in the MEIMD for structures in horizontal direction.

Acknowledgments

This research is financially supported by National Natural Science Foundation of China with granted number 50508010, Jiangsu Province Natural Science Foundation with granted number BK2008282, Program for New Century Excellent Talents of the Ministry of Education in China, the Program for Jiangsu Province 333 Talents, and the Project-sponsored by SRF for ROCS, SEM. These supports are gratefully acknowledged.

References

[1] G.W. Housner, et al., Structural control: past, present, and future, *ASCE Journal of Engineering Mechanics* 123 (9) (1997) 897–971.
[2] U. Aldemir, M. Bakioglu, Active structural control based on the prediction and degree of stability, *Journal of Sound and Vibration* 247 (4) (2001) 561–576.
[3] R. Guclu, H. Yazici, Vibration control of a structure with ATMD against earthquake using fuzzy logic controllers, *Journal of Sound and Vibration* 318 (1–2) (2008) 36–49.
[4] H. Alli, O. Yakut, Application of robust fuzzy sliding-mode controller with fuzzy moving sliding surfaces for earthquake-excited structures, *Structural Engineering and Mechanics* 26 (5) (2007) 517–544.
[5] T. Shimada, J. Suhara, Three dimensional seismic isolation system for next-generation nuclear power plant with rolling seal type air spring and hydraulic rocking suppression system, *Proceedings of the ASME Pressure Vessels and Piping Conference*, Vol. 8, Denver, Colorado, USA, 2005, pp. 183–190.
[6] G.C. Lee, K.C. Chang, G.C. Yao, Dynamic behavior of a prototype and a 2/5 scale steel frame structure, *Proceedings of Fourth US National Conference on Earthquake Engineering*, Vol. 2, California, 1990, pp. 605–613.
[7] R.C. Lin, Z. Liang, T.T. Soong, R.H. Zhang, An experimental study on seismic behavior of viscoelastically damped structures, *Engineering Structure* 13 (1) (1991) 75–84.
[8] J.M. Bracci, A.M. Reinhorn, J.B. Mander, Seismic resistance of reinforced concrete frame structures designed only for gravity loads: Part III—experimental performance and analytical study of a structural model, Technical Report NCEER-92-0029, National Center for Earthquake Engineering Research, University at Buffalo, 1992.
[9] K.C. Chang, M.L. Lai, T.T. Soong, D.S. Hao, Y.C. Yeh, Seismic behavior and design guidelines for steel frame structures with added viscoelastic dampers, Technical Report NCEER-930009, State University of New York at Buffalo Department of Civil Engineering, 1993.
[10] K.C. Chang, S.J. Chen, M.L. Lai, Inelastic behavior of steel frames with added viscoelastic dampers, *ASCE Journal of Structural Engineering* 122 (10) (1996) 2456–2467.
[11] J.P. Ou, X.Y. Zou, Experiment and analysis study on seismic vibration-suppressed effects of viscoelastic energy dissipation on steel high-rise structure, *Journal of Harbin University of Architecture* 32 (4) (1999) 1–6 (in Chinese).
[12] Z.D. Xu, Earthquake mitigation study on viscoelastic dampers for reinforced concrete structures, *Journal of Vibration and Control* 13 (1) (2007) 29–45.
[13] K.W. Min, J.K. Kim, S.H. Lee, Vibration tests of 5-storey steel frame with viscoelastic dampers, *Engineering Structures* 26 (2004) 831–839.
[14] K.C. Chang, Y.Y. Lin, Seismic response of full-scale structure with added viscoelastic dampers, *ASCE Journal of Structural Engineering* 130 (4) (2004) 600–608.

[15] C. Chen, W. Xu, Earthquake simulation tests on a weak-layer steel frame equipped with EDD, *World Earthquake Engineering* 22 (4) (2006) 121–126 (in Chinese).
[16] Z.D. Xu, *Structure Dynamics*, China Science Press, Beijing, 2007 (in Chinese).
[17] X. Zeng, Experimental Study on the Structure with Multi-Dimensional Earthquake Isolation and Mitigation Devices Under Horizontal Earthquake, Thesis of Master Degree in Southeast University, 2007 (in Chinese).
[18] A.K. Chopra, *Dynamics of Structures Theory and Applications to Earthquake Engineering*, Pearson Education Inc., USA, 2001.